Dynamic modelling of an Ammonia to Power application at high efficiency using a solid oxide fuel cell system

Michele Bolognese¹ Emanuele Martinelli¹ Luca Pratticò¹ Matteo Testi¹

¹Fondazione Bruno Kessler, Italy, mbolognese@fbk.eu

Abstract

Ammonia is a promising zero carbon and sustainable hydrogen carrier that can be used as a fuel in solid oxide fuel cells (SOFC) by offering advantages related to the ease of storage and the possibility of being used directly without an external reformer. In this study, a Modelicabased dynamic model of an 'Ammonia to Power' (A2P) system was developed by integrating ammonia decomposition kinetics, electrochemical reactions, all the systemlevel components and the main control loops. A novel Balance of Plant (BoP) configuration is proposed, featuring a five-way heat exchanger that recovers waste heat primarily using the fuel stream as the thermal energy vector instead of air. The model evaluates transient responses to operational perturbations, the behavior of the different control loops, and recirculation percentage rates to optimize system performance. Efficiency is calculated as the ratio of the power output from the SOFC to the power derived from the fresh ammonia line.

Keywords: SOFC, Ammonia, BoP, High temperature fuel cell

1 Introduction

The sustainable energy transition needs carbon-neutral solutions to meet the worldwide increasing energy demand (16 TW in 2010 to 23 TW in 2030 and 30 TW in 2050) while minimizing the environmental impacts (Dresselhaus and Thomas 2001). In this contest, green hydrogen produced from renewable energy sources (RES) plays a crucial role and is considered a potential alternative to fossil fuels. However, the establishment of a hydrogen economy faces substantial hurdles that must be addressed. Beyond the necessity of large-scale production of renewablebased green hydrogen, there are also long-standing challenges related to transportation, distribution, storage, and end-use of hydrogen that need a solution. Therefore, it is essential to develop innovative and effective strategies that can facilitate sustainable energy transition. In this perspective, the potential of utilizing ammonia as a hydrogen carrier for on-site power generation via ammonia decomposition is systematically discussed (Zhai et al. 2023). Hydrogen possesses a high gravimetric energy density of approximately 120 MJ/kg, surpassing conventional fuels like gasoline (44 MJ/kg) but the volumetric energy density of hydrogen is lower, so it requires larger vessels for storage

technologies have been explored for the dense storage of hydrogen but physical processes such as liquefaction and compression, which are used for storage and transportation, are energy intensive. For instance, hydrogen liquefaction consumes about 13.8 kWh/kg of liquid hydrogen, which corresponds to approximately 40% of hydrogen's energy content (Zhang et al. 2023). Similarly, hydrogen compression to high pressures, such as 700 bar, is essential for applications like fuel cell vehicles to achieve acceptable storage compactness. This process is energyintensive; for instance, a study reported that using multiple pressure stages in refueling stations can reduce compressor power consumption by 17%, highlighting the significant energy demands of hydrogen compression. On the other hand, material-based storage, such as zeolites and metal hydrides, can provide a hydrogen storage capacity of up to 13 wt%., but these technologies often face challenges related to technological readiness levels (TRL). Higher energy densities are obtained with hydrogen storage in the form of chemicals such as methanol (12.5 wt %) or ammonia (17.65 wt%). Ammonia (NH₃) has emerged as a promising hydrogen carrier and carbon-free fuel, offering a unique combination of high hydrogen content, established global infrastructure, and compatibility with various energy conversion technologies. Historically, the ammonia synthesis via the Haber-Bosch (HB) process has been fundamental in worldwide agriculture and industry, by enabling the large-scale ammonia production via nitrogen and grey hydrogen produced via steam methane reforming, under high temperature and pressure operating conditions. The potential of ammonia as an energy carrier spans multiple applications, including internal combustion engines (ICE (Tornatore et al. 2022)), gas turbines (Pashchenko 2024a), and fuel cells (Pashchenko 2024a; Qi et al. 2023; Pashchenko 2024b). Among these, solid oxide fuel cells (SOFCs) stand out for their ability to utilize ammonia directly as a fuel, bypassing the need for external hydrogen production or cracking processes. This direct utilization enables SOFC systems to achieve high power densities while producing only nitrogen and water as byproducts, aligning with the goals of a sustainable energy future (Dhawale et al. 2023). Several authors studied the configurations of direct ammonia SOFC system and their performance (Cinti et al. 2016; Nemati et al. 2025; Ayerbe et al. 2024). In their work, Cinti et al. have demon-

and transportation. Different physical and material-based

strated the improved efficiency of a direct ammonia SOFC system if compared to a hydrogen-based one. Nemati et al. have shown the importance of the anode off-gas recirculation and pre-cracking to improve the efficiency and reduce the impact of nitriding. The dynamic behavior of the A2P BoP is notably complex due to the interaction among its various functional zones, subcomponents, and control loops. This study addresses this challenge by developing a comprehensive dynamic model in Modelica language, serving as a prototyping tool that enables the analysis of overall system performance, including the direct ammonia solid oxide electrolyzer, the external cracker, and the waste heat recovery system under various operating scenarios. Additionally, the incorporation of advanced control loops and recirculation strategies offers new insights into the system-wide dynamics and operational stability, contributing novel understanding to the field of P2A plant integration and control

2 Methodology

Dynamic modeling is crucial to understanding and optimizing the behavior of an energy system balance of a plant under different operational conditions by simulating complex interactions between the system components. Dynamic modeling activities can also be a useful guide for the development of a control strategy to enhance overall system efficiency, flexibility, and reliability. Modern process modeling has evolved beyond simple material and energy balance calculations to become a strategic tool for managing and better understanding the potential of prototypes by gaining a competitive advantage (Ayerbe et al. 2024). Robust models enable rapid adaptation to market changes and serve as repositories of corporate knowledge. Models also capture valuable experimental data that aid in process optimization, redesign, and patent development. This creates a continuous improvement cycle in which each use enhances the value of the model, increasing the return on investment, and driving innovation. The Modelica language (Mattsson and Elmqvist 1997; Qiu et al. 2024) enables the simulation of complex systems such as the balance of plant (BoP) of hydrogen systems by using non-causal modeling, reusable components, and equation-based formulation. Non-causality allows the same equations to be used for forward and inverse kinematics, enhancing adaptability across engineering applications. In addition, the use of proper media for the fuel and air stream ensures accurate thermodynamic property calculations that are fundamental for calculating a heat and material balance that gives crucial information regarding the design of the overall system. In this study, one-dimensional equidistant discretizations is applied to each component of the BoP model. Furthermore, diffusion phenomena were neglected by simplifying the simulation.

2.1 BoP Model Description

This work presents the development of an 'Ammonia to Power' (A2P) plant model based on solid oxide fuel cell

technology, which incorporates all other components of the system. In Figure 1, the functional Process and Instrumentation Diagram (P&ID) is presented:

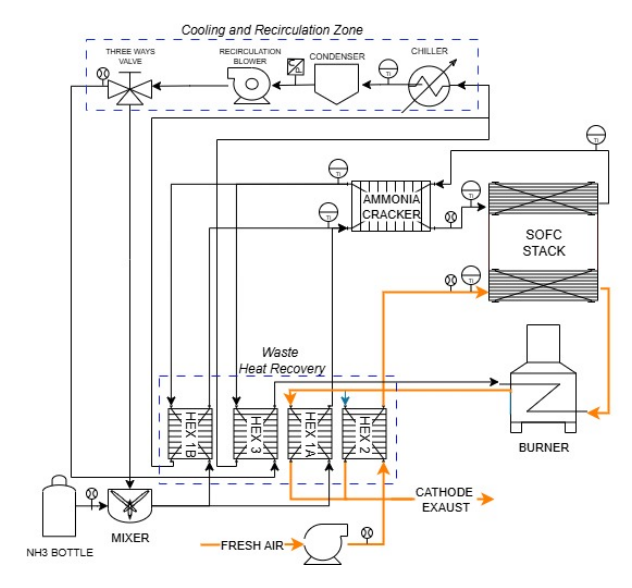


Figure 1. Functional Process and Instrumentation Diagram (P&ID) with fuel loop (black line) and air loop (orange line)

In the P&ID, the air flow loop is identified in orange, while the fuel flow loop appears in black. Each component is clearly labeled, and the regions associated with the waste heat recovery system, as well as the fuel cooling and recirculation circuits, are marked with dashed outlines for easy identification. To contribute to the development of an efficient and sustainable ammonia-based energy solution, this study aims to provide information on system design, operation, and control strategies. The key core of the system is represented by a solid oxide fuel cell stack, but particular attention was paid to the waste heat recovery and recirculation aspect of the anode off-gas within the AMON project. In Figure 2, the layout of the BoP model is presented using the Modelon Impact (Modelon 2025) interface.

From the layout in Figure 2, it is possible to distinguish the hot BOP that works at high temperature from the cold BOP starts from the condenser (block 6) and finishes downstream of the recirculation blower (block 9). Moreover, it is possible to also notice that other components of the Modelon library (joints and splits) were used to couple and split the fuel and air streams in the Hot BoP.

The BoP components in Figure 2 are numbered and described in the following.

1) Stack

The stack model is based on the Fuel Cell library (Andersson et al. 2011) by Modelon Impact (*Fuel Cell Library* 2025; Modelon 2025). The model was modified by implementing ammonia cracking in the anode channel. The stack model was validated by considering the polarization curves obtained in FBK test benches for other works within the AMON project. Moreover, to the stack an ac-

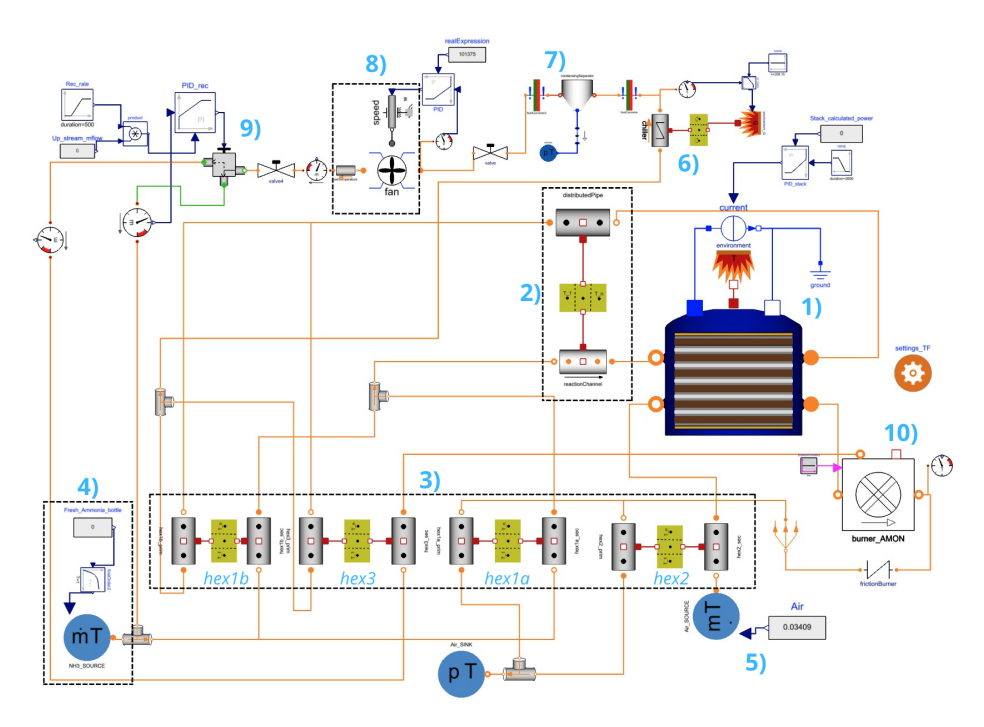


Figure 2. Layout of Ammonia to Power BoP model in Modelon Impact.

tive control loop based on a PID that controls the current delivered by the stack is applied in order to control the desired power for the different operating modes.

2) External Cracker

The External Cracker model is based on the use of the Modelon Standard Library by using the reaction channel and distributed pipe model that are connected to the metal wall model in counterflow mode.

3) Heat Exchanger Network

The model of the heat exchanger network is based on 4 heat exchangers that are calibrated according to the technical datasheet provided within the AMON project. In addition, several split and joint components of the Modelon library were used to modify the mass flow rates of the four different HEXs. In particular, air, which typically serves as the thermal carrier for the high-temperature balance of plant (BoP) components in SOC technologies, is used only 10% to preheat the recirculated fuel mixture (NH₃ and N₂), while the remaining portion is used to preheat the air entering the stack. Each heat exchanger (HEX) consists of a distributed pipe connected to a metal wall.

4) Fresh Ammonia Sourcer

This is an ideal ammonia source model at 25 °C and the ammonia mass flow rate required by the system is calculated as a function of the current delivered from the stack and the utilization of the fuel:

$$\dot{m}_{\rm NH_3} = \frac{n_{\rm cell}I}{2U_{\rm fuel}F} \frac{2}{3}MM_{\rm NH_3} \tag{1}$$

where n_{cell} is the number of cells in the stack, I is the current, U_{fuel} is the fuel utilization (equal to 0.7), F is the

Faraday constant and $MM_{NH_3} = 0.017031 \,\mathrm{kg/mol}$ is the molecular weight of ammonia.

5) Air Source

This is an ideal air source model at 25 °C with the mass flow rate defined as follows:

$$\dot{m}_{Air} = \frac{n_{cell}I}{4U_{Air}F} Y_{O_2} MM_{Air}$$
 (2)

where $U_{\rm Air}$ is air utilization (equal to 0.11), $Y_{\rm O_2}$ is the oxygen content of the air (0.2094%) and $MM_{\rm Air} = 0.028965\,{\rm kg/mol}$ is the molecular weight of the air.

6) Chiller

The chiller is an ideal and simplified model of a simple pipe connected to a thermal power source that chills the Off Gas Anode (AOG) to 25 ° C using a specific PID component to modulate the cooling power required.

7) Condenser

The Condensing Separator model is a Modelon library component based on a condensing volume that efficiently separates water from a generic gas stream. A specific condensate medium is used by implementing two medium converters that can couple the medium used for the fuel and the condensate one.

8) Recirculation Blower

This is a simplified model of an axial fan in which the characteristics of the fan with respect to the volume flow rate $V_{\rm flow}$ and the power absorbed by the fan $P_{\rm fan}$, have been implemented as follows:

Moreover, a time constant τ affects the equations that govern the mass flow rate (m_{flow}) and power consumption (P) as can be seen in the following equations:

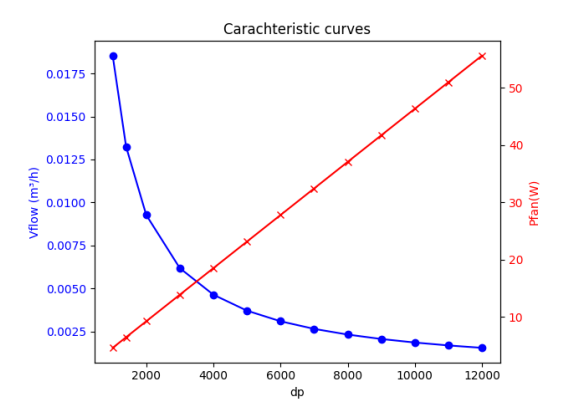


Figure 3. Characterization curves of the recirculation fan

$$\tau \frac{dm_{\text{flow}}}{dt} + m_{\text{flow}} = V_{\text{flow}_{\text{in}}} dA_{\text{inflow}}$$
 (3)

$$\tau \frac{dP}{dt} + P = P_{\text{fan}_{\text{in}}} \tag{4}$$

where dA_{inflow} is the mass density calculated in the mass port upstream of the component.

The speed of the recirculation blower is controlled by a PID controller to maintain the upstream pressure higher than the environmental pressure during transitions between different operating modes.

9) 3-Ways recirculation valve

This three-way valve model is designed for single-phase medium applications and belongs to the ThermalPower 1.28 library of Modelon (Modelon 2025). The valve assumes turbulent, non-choked flow with static mass and energy balances and no actuator dynamics. By default, the flow characteristic is linear, but can be customized.

10) Ammonia Catalytic burner

The burner model is a fixed volume combustion chamber of the Modelon library. In this study, it was modified according to the A2P system by replacing fossil fuels with a mixture of hydrogen (H_2) and ammonia (NH_3) . Energy calculations use the Lower Heating Value (LHV) of the H_2/NH_3 blend.

3 Main processes

In this section, the main processes implemented in the A2P dynamic model are described. A particular medium NASA-based of 5 elements (H₂, NH₃, H₂O, N₂, O₂) was created to implement Ammonia in the fuel composition.

3.1 Ammonia cracking Processes

For ammonia cracking, the studies by Kishimoto et al. (Kishimoto et al. 2017) and Lucentini et al. (Lucentini et al. 2021) were considered. The model of Kishimoto et al. was applied to the cracking of ammonia within the anode channel of the stack (block 1), as they developed

an experimentally validated ammonia decomposition reaction ($R_{\rm kish}$) for a Ni-YSZ anode. The reaction model developed by Lucentini et al. ($R_{\rm luc}$) for the decomposition of ammonia over Ni-Ru supported on CeO₂ was applied to the external cracker reaction channel (block 2). The following equations present the ammonia degradation reaction rates for both the stack and the external reformer:

$$R_{\text{kish}} = S_{\text{Ni-pore}} A^{\text{Ni-pore}} \exp\left(-\frac{E}{RT}\right) p_{\text{NH}_3}^a \left(p_{\text{H}_2} + c\right)^b$$
 (5)

$$R_{\text{luc}} = \frac{kK_1C_{\text{NH}_3}}{\left(1 + K_1C_{\text{NH}_3} + \sqrt{\frac{C_{\text{H}_2}}{K_4}}\right)^2}$$
(6)

In this study, the materials constituting the storage cell and the cracker catalyst are not yet defined, so the same materials of the reference papers were considered by using the same values of the coefficients for the two reaction rates. Subsequently, the ammonia decomposition reaction of Lucentini et al. is calibrated considering the coefficient values valid for 5Ni1Ru/CeO₂ by implementing the geometric characteristics of the cracker presented in Table 1, which refers to the equivalent diameter of the pipe having the same cross section as the rectangular channel of the cracker plates.

Table 1. Technical specifications of the external cracker

Parameters	Value	Unit	Description
$n_{ m plates}$	34	_	Number of plates
$A_{ m heat}$	0.4	m^2	Heat exchange area
length	20.7	cm	Total length
height	13.7	cm	Total height
width	7.7	cm	Total width
d_{eq}	2.5	cm	Equivalent diameter
$arepsilon_{ m bed}$	0.245	_	Porosity of the bed
f_v	0.196	_	Catalyst volume fraction

In this study, the external cracker was considered as a fixed-bed reactor; thus, the concentration of ammonia and hydrogen is calculated only over the void volume. The amount of catalyst needed within the reactor bed (g_{cat} [g]) depends on the temperature and the conversion percentage, as shown in Figure 4.

3.2 Electrochemical Process

In this study, the structure of the stack model is based on the Modelon Fuel Cell Library, which utilizes the coupling between the anode channel, the elementary cell, and the cathode channel. Within the elementary cell, a simplified equivalent electrical circuit was used to characterize the polarization curves of the simulation by comparing them with the experimental data obtained at the FBK test bench using a short stack of 6 cells provided by Solydera. More

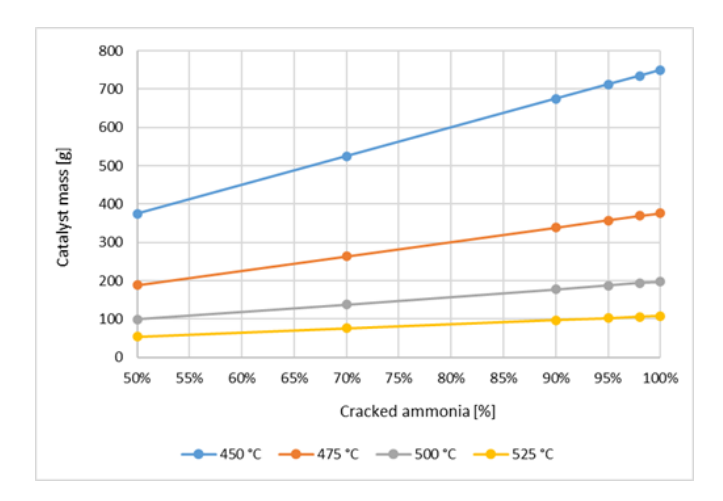


Figure 4. Ammonia cracking percentage as a function of temperature and mass of the catalyst.

details of these validation activities are presented in another FBK study at the Modelica Conference.

Taking into account the desired rangeability of the operating conditions of the A2P system within the AMON project, the cell voltage in the cell model was calculated by considering only ohmic losses.

$$V_{\text{cell}} = E_0 - \text{ASR}(T) j_{\text{cell}} \tag{7}$$

where E_0 is the Nernst voltage, j_{cell} is the current density, and ASR is the area specific resistance calculated as follows:

$$E_0 = \frac{1}{n_e F} \left(\Delta g_{\text{reaction}} + RT_{\text{cell}} \ln \left(\frac{p_{\text{H}_2} o}{p_{\text{H}_2} p_{\text{O}_2}^{0.5}} \right) \right)$$
(8)

$$ASR(T) = ASR_0 + \exp\left[\frac{E_a}{R}\left(\frac{1}{T_{\text{cell}}} - \frac{1}{T_0}\right)\right]$$
 (9)

$$j_{\text{cell}} = \frac{I}{A_{\text{cell}}} \tag{10}$$

For this work, a value of $ASR_0 = 0.34 \times 10^{-4} \Omega/cm^2$ and an activation energy $E_a = 24.8 \times 10^3 \, \text{kJ/mol}$ were used with a reference temperature $T_0 = 600$ °C, obtaining a relative error less than 3%, consistent with previous work on SOC technologies performed in other EU projects.

3.3 **Condensation Process**

The condensation process follows a first-order differential equation governed by the condensation time constant τ_{sat} . This parameter controls the rate at which water vapor condenses into liquid and is defined as follows:

$$\tau_{\text{sat}} \frac{d}{dt} \dot{m}_{\text{water}} + \dot{m}_{\text{water}} = \dot{m}_{\text{feed}} (X_{\text{feed}} - X_{\text{sat}}) + k_{\text{molar}} \max(\varepsilon - \dot{m}_{\text{water}}, y_{H_2O} - y_{\text{sat}})$$
(11)

Table 2. Stack Technical Parameters

Parameters	Value
Active Area [cm ²]	320
Number of cells	80
Max Current [A]	128
Fuel Utilization [%]	70
Max Power [kW]	8

where

- X_{feed} is the water mass fraction in the inlet stream,
- X_{sat} is the saturated water mass fraction, calculated

$$X_{\text{sat}} = \frac{y_{\text{sat}}}{1 - y_{\text{sat}}} \cdot k_{\text{molar}} \cdot (1 - X_{\text{feed}})$$
 (12)

where y_{sat} is the saturated mole fraction of water vapor calculated as a function of temperature T and pressure p:

$$y_{\text{sat}} = \frac{p_{\text{sat}}(T)}{p} \tag{13}$$

Here, $p_{\text{sat}}(T)$ the saturation pressure is calculated as a function of temperature and is a medium parameter.

The factor of molar ratio k_{molar} is calculated as the ratio of the molar fraction of water to the molar fraction of gas without water:

$$k_{\text{molar}} = \frac{MM_{H_2O}}{MM_{H_2\text{dry_gas}}} \tag{14}$$

Combustion of H_2 / NH_3 mixture

In the burner model, the following oxidation reactions for H₂ and NH₃ have been integrated into the combustion reaction by implementing a specific stoichiometric matrix:

$$H_2 + \frac{1}{2}O_2 \to 2H_2O$$
 (15)

$$NH_3 + \frac{3}{4}O_2 \rightarrow \frac{3}{2}H_2O + \frac{1}{2}N_2$$
 (16)

These reactions assume ideal conditions under the assumption of complete combustion, where all reactants are fully converted into products, primarily water vapor and nitrogen gas, with no unburned residues or intermediate species.

3.5 **Heat Recovery System**

In this study, particular attention was paid to the heat recovery system of the thermal energy coming from the high $+k_{\text{molar}} \max(\varepsilon - \dot{m}_{\text{water}}, y_{H_2O} - y_{\text{sat}})$ temperature SOFC and the additional burner. The heat heat recovery system is composed of 4 heat exchangers:

- hex1a (fuel-fuel): preheating of the recirculated fuel and fresh ammonia mixture by using the 50% of mass flow rate of anode fuel from the stack after the heating of the external cracker
- hex1b (fuel-fuel): preheating of the non-recirculated fuel that feeds the burner by using the 50% of mass flow rate of anode fuel from the stack after the heating of the external cracker
- hex2 (fuel-air): preheating of the recirculated fuel and fresh ammonia mixture by using the 10% of exhaust gas mass flow rate from the burner
- hex3 (air-air): preheating of fresh air by using the 90% of exhaust gas mass flow rate from the burner

All the HEXs mentioned above are in counterflow configuration; the specific geometries were implemented coherently with the design data of the AMON project. In the following figure is possible to see the trends of hot and cold fuels vs the longitudinal distance of each heat exchanger.

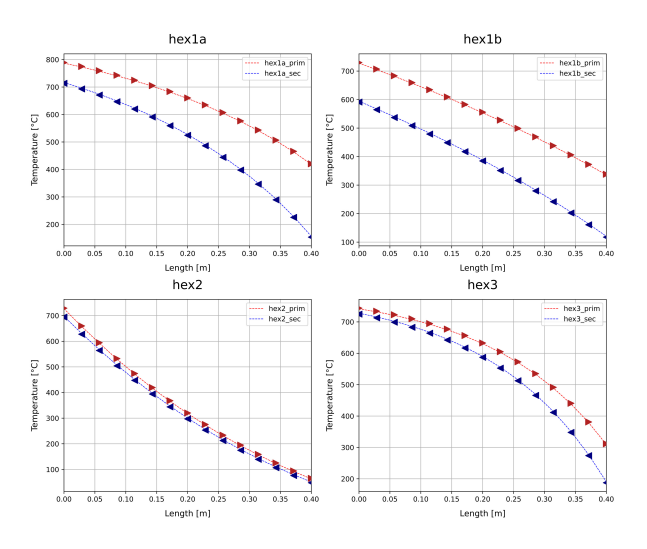


Figure 5. Trends of temperature of hot and cold sides vs distance for each HEX.

Figure 5 shows the temperature profiles along the length of four heat exchanger configurations (hex1a, hex1b, hex2, hex3), illustrating heat transfer between primary and secondary fluids. The decreasing primary and increasing secondary temperature trends suggest counterflow or parallel flow behavior, influenced by variations in the design of the heat exchanger and operating conditions.

4 Results

In this section, the main results of the BoP model are presented. An initial simulation of 200,000 seconds was performed, with an elapsed time of approximately 14 to 15 minutes, to verify the behavior of the external reformer. Setting a fuel recirculation rate at 88 % and a power at 8 kW (nominal condition). In Figure 6, it is possible to

see that during the simulation time, the NH₃ conversion rate of the external reformer and the related trends of NH₃ molar fraction and inlet/outlet fuel temperatures reaches converge and the outlet NH₃ molar fraction is around 3% in a consistent way with the decision-making decisions made during the design phase of the system for the AMON project.

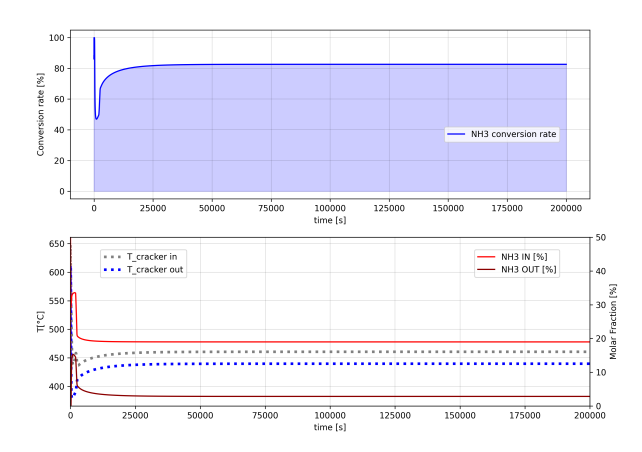


Figure 6. External cracker behaviors at nominal condition with 88 % of recirculation rate. Ammonia conversion rate [%] (upper plot), inlet and outlet cracker fuel temperature, and NH₃ molar fraction (lower plot)

Eventually, considering the same simulation, the relative pressure profiles of air (blue line) and fuel (red line) are presented in Figure 6.

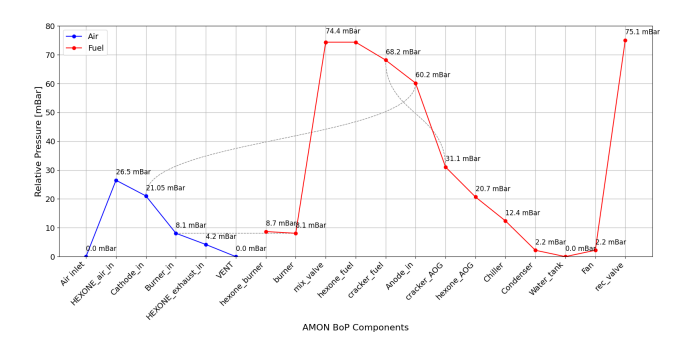


Figure 7. Pressure drops trends for all the components of the BoP model [air channel in blue and fuel channel in red]

It can be observed that the fuel pressure profile is higher than that of air, with a recorded pressure difference of approximately 39 mbar under nominal conditions (8 kW) in this simulation. This configuration ensures that the anode pressure at the stack inlet is higher than the cathode stack pressure, which is a crucial safety measure to prevent backflow or mixing risks. The fuel loop achieves a peak pressure of 74.4 mbar through fan-driven circulation, with a pre-recirculation pressure drop of approximately 73 mbar. This results in a recirculation rate of 88%, while 12% is directed to the burner. On the other hand, the air pressure profile achieves a maximum pressure of 26.5 mbar upstream of the heat recovery system. Afterward, a short sensitivity analysis of the fuel mass flow rate recircu-

lation rate was performed to select the best configuration. The fuel that is recirculated after the cracking, electrolysis process, chilling, and condensation is a mixture mainly composed of N_2 . In Table 4, four different cases with a recirculation rate of 80, 85, 88, and 90 % have been evaluated.

Considering the design decisions made during the design phase of the system, the 88% fuel recirculation rate was chosen as the optimal solution because it allows the recirculation of the blower operation to be respected in terms of the maximum flow rate and achieves an efficiency of 73.13%, which is above the 70% target of the AMON project.

Finally, in Figure 8, the transitions between full load (8 kW) and partial mode (2.4 kW) were simulated in order to verify the behaviors of the control loops dedicated to the modulation of current for the power control of the stack, the control of the AOG recirculation (CL_fan) by modulating the rpm [Hz] of the blower, and the control of opening/closing of the 3-way valve (CL_3ways). Moreover, in the same figure it is possible to see the trend of the overall efficiency of the system, which is calculated as follows:

$$\eta_{\text{BoP}} = \frac{P_{\text{stack}}}{LHV_{NH_3} \cdot \dot{m}_{NH_3,in}}$$
(17)

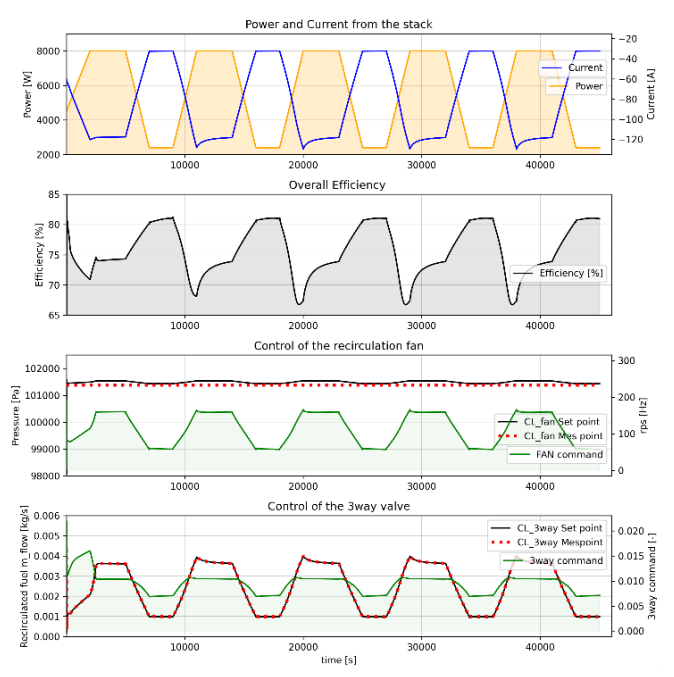


Figure 8. Dynamic simulation results of Full to Partial Mode transitions: Power and Current of the stack (upper), Overall Efficiency of the system (medium-high), Control of recirculation fan (medium-low), and Control of the 3-way valve (lower plot).

It is possible to see that the control of the stack power by modulating the current is quite stable. However, during the transition from partial to full operation, the overall efficiency of the system experiences a transient decrease. This initial drop in efficiency occurs only in the first moments after the switch, but subsequently stabilizes within the typical range associated with full load operation, which was previously calculated as approximately 72–74%.

Moreover, the CL_3ways control loop governing the 3-way valve demonstrates consistent stability, while the CL_fan control loop for the recirculation fan shows minor deviations from the set point (around 200 Pa). These deviations are sufficiently small to be considered negligible, so the control loop can be considered to function correctly by maintaining the required pressure set point. Overall, despite some small adjustments required, the control strategy implemented in the model exhibits robust stability and good dynamic response, ensuring reliable operation under varying load conditions.

5 Conclusion

This work presents a description and comprehensive analysis of a Modelica-based dynamic model of an Ammonia2Power (A2P) system utilizing the coupling of a direct ammonia solid oxide fuel cell and an external reformer. With the integration of detailed ammonia decomposition with different catalysts for the external reformer and the stack, the electrochemical processes, and an innovative BoP addressing enhanced waste heat recovery, the model enables in-depth analysis of system behavior under different operating modes. Two different simulations were performed, one addressed to calculate heat and material balance (after 200000 s of stationary behavior) and one dedicated to the transitions between full and partial modes. Furthermore, the simulation results demonstrate that the proposed system can achieve a high ammonia conversion rate and efficient heat recovery, with an AOG recirculation rate of 88% and stable operation in full (8 kW) and partial (2.4 kW) modes. The pressure profile of both fuel and air streams was calculated, ensuring safe operation by maintaining anode pressure higher than the cathode pressure, minimizing backflow risks. Finally, the dynamic Modelica-based modeling approach provides valuable insights into the transient behavior of the system, the impact of AOF recirculation and heat integration on the overall efficiency of the system, and the effectiveness of control strategies. This study confirms the technical feasibility and potential of ammonia as a vector and hydrogen carrier for direct utilization in SOFC BOP. The model acts as a robust tool to guide the design phase of the prototype and the optimization of future A2P systems, supporting the transition to sustainable energy and carbon-neutral solutions. Future work will focus on the implementation of a proper state machine for the control strategy, further refinements of control loops, and verification of emergency scenarios to evaluate system safety in order to enhance system flexibility and reliability under real-world operating conditions.

Case 1	Case 2	Case 3	Case 4
80%	85%	88%	90%
12.492	15.12	17.856	20.628
230	239	241	244
71.20	73.30	74.40	75.01
2.16	2.11	2.08	2.06
46.96	56.99	72.94	95.49
93.91	92.94	83.00	84.51
3.95	3.23	2.85	2.48
1.6e - 6	0.002	0.05	0.17
0.0310	0.0308	0.0306	0.0305
1.007	1.219	1.407	1.603
	80% 12.492 230 71.20 2.16 46.96 93.91 3.95 1.6e-6 0.0310	80% 85% 12.492 15.12 230 239 71.20 73.30 2.16 2.11 46.96 56.99 93.91 92.94 3.95 3.23 1.6e-6 0.002 0.0310 0.0308	80% 85% 88% 12.492 15.12 17.856 230 239 241 71.20 73.30 74.40 2.16 2.11 2.08 46.96 56.99 72.94 93.91 92.94 83.00 3.95 3.23 2.85 1.6e-6 0.002 0.05 0.0310 0.0308 0.0306

Table 3. Sensitivity Analysis for Different Recirculation Rates (80, 85, 88, 90%)

Acknowledgements

The project is supported by the Clean Hydrogen Partnership and its members, Hydrogen Europe and Hydrogen Europe Research, under Grant Agreement No. 101101521.

References

Andersson, Daniel, & Aring, Erik Berg, Jonas Eborn, Jinliang Yuan, Sundé, and Bengt N (2011-06). "Dynamic modeling of a solid oxide fuel cell system in Modelica". en. In: URL: https://ep.liu.se/en/conference-article.aspx?series=ecp&issue=63&Article_No=66 (visited on 2025-04-15).

Ayerbe, Cécile, Caroline Boulos, and Francesco Castellaneta (2024-09). "Navigating protection mechanisms and innovation models: A literature-based configurational framework of intellectual property strategies". In: *Technovation* 137, p. 103101. ISSN: 0166-4972. DOI: 10.1016/j.technovation. 2024.103101. URL: https://www.sciencedirect.com/science/article/pii/S0166497224001512 (visited on 2025-04-15).

Cinti, G., G. Discepoli, E. Sisani, and U. Desideri (2016). "SOFC operating with ammonia: Stack test and system analysis". In: *International Journal of Hydrogen Energy* 41.31, pp. 13583–13590. ISSN: 0360-3199. DOI: https://doi.org/10.1016/j.ijhydene.2016.06.070. URL: https://www.sciencedirect.com/science/article/pii/S036031991630595X.

Dhawale, Dattatray S., Saheli Biswas, Gurpreet Kaur, and Sarbjit Giddey (2023). "Challenges and advancement in direct ammonia solid oxide fuel cells: a review". en. In: *Inorganic Chemistry Frontiers* 10.21, pp. 6176–6192. ISSN: 2052-1553. DOI: 10.1039/D3QI01557B. URL: https://xlink.rsc.org/DOI=D3QI01557B (visited on 2025-04-15).

Dresselhaus, M. S. and I. L. Thomas (2001-11). "Alternative energy technologies". en. In: *Nature* 414.6861, pp. 332–337. ISSN: 0028-0836, 1476-4687. DOI: 10.1038/35104599. URL: https://www.nature.com/articles/35104599 (visited on 2025-04-15).

Fuel Cell Library (2025). en-US. Publication Title: Modelon. URL: https://modelon.com/library/fuel-cell-library/ (visited on 2025-04-15).

Kishimoto, Masashi, Naoto Furukawa, Tatsuya Kume, Hiroshi Iwai, and Hideo Yoshida (2017-01). "Formulation of ammonia decomposition rate in Ni-YSZ anode of solid oxide fuel cells". In: *International Journal of Hydrogen Energy* 42.4,

pp. 2370–2380. ISSN: 0360-3199. DOI: 10.1016/j.ijhydene. 2016.11.183. URL: https://www.sciencedirect.com/science/article/pii/S0360319916335169 (visited on 2025-04-15).

Lucentini, Ilaria, Germán García Colli, Carlos D. Luzi, Isabel Serrano, Osvaldo M. Martínez, and Jordi Llorca (2021-06). "Catalytic ammonia decomposition over Ni-Ru supported on CeO2 for hydrogen production: Effect of metal loading and kinetic analysis". In: *Applied Catalysis B: Environmental* 286, p. 119896. ISSN: 0926-3373. DOI: 10.1016/j.apcatb. 2021.119896. URL: https://www.sciencedirect.com/science/article/pii/S0926337321000229 (visited on 2025-04-15).

Mattsson, Sven Erik and Hilding Elmqvist (1997-04). "Modelica - An International Effort to Design the Next Generation Modeling Language". en. In: *IFAC Proceedings Volumes* 30.4, pp. 151–155. ISSN: 14746670. DOI: 10.1016/S1474-6670(17)43628-7. URL: https://linkinghub.elsevier.com/retrieve/pii/S1474667017436287 (visited on 2025-04-15).

Modelon (2025). *Modelon Impact*. https://modelon.com/modelon-impact/. Accessed: 2025-07-18.

Nemati, Arash, Hossein Nami, Javid Beyrami, Rafael Nogueira Nakashima, and Henrik Lund Frandsen (2025). "Efficient and durable system design for ammonia-fueled solid oxide fuel cells using multiscale multiphysics modeling approach". In: *Fuel* 392, p. 134837. ISSN: 0016-2361. DOI: https://doi.org/10.1016/j.fuel.2025.134837. URL: https://www.sciencedirect.com/science/article/pii/S0016236125005617.

Pashchenko, Dmitry (2024a-03). "Ammonia fired gas turbines: Recent advances and future perspectives". In: *Energy* 290, p. 130275. ISSN: 0360-5442. DOI: 10.1016/j.energy.2024. 130275. URL: https://www.sciencedirect.com/science/article/pii/S036054422400046X (visited on 2025-04-15).

Pashchenko, Dmitry (2024b-03). "Ammonia fired gas turbines: Recent advances and future perspectives". In: *Energy* 290, p. 130275. ISSN: 0360-5442. DOI: 10.1016/j.energy.2024. 130275. URL: https://www.sciencedirect.com/science/article/pii/S036054422400046X (visited on 2025-04-15).

Qi, Yunliang, Wei Liu, Shang Liu, Wei Wang, Yue Peng, and Zhi Wang (2023-10). "A review on ammonia-hydrogen fueled internal combustion engines". In: *eTransportation* 18, p. 100288. ISSN: 2590-1168. DOI: 10.1016/j.etran.2023. 100288. URL: https://www.sciencedirect.com/science/article/pii/S2590116823000632 (visited on 2025-04-15).

Qiu, Kaiying, Junlu Yang, Zhi Gao, and Fusuo Xu (2024-04). "A review of Modelica language in building and energy: Development, applications, and future prospect". In: *Energy and*

- Buildings 308, p. 113998. ISSN: 0378-7788. DOI: 10.1016/j. enbuild.2024.113998. URL: https://www.sciencedirect.com/science/article/pii/S0378778824001142 (visited on 2025-04-15).
- Tornatore, Cinzia, Luca Marchitto, Pino Sabia, and Mara De Joannon (2022-07). "Ammonia as Green Fuel in Internal Combustion Engines: State-of-the-Art and Future Perspectives". English. In: *Frontiers in Mechanical Engineering* 8. ISSN: 2297-3079. DOI: 10.3389/fmech.2022.944201. URL: https://www.frontiersin.org/tjournals/mechanical-engineering/articles/10.3389/fmech. 2022.944201/full (visited on 2025-04-15).
- Zhai, Lingling, Shizhen Liu, and Zhonghua Xiang (2023). "Ammonia as a carbon-free hydrogen carrier for fuel cells: a perspective". en. In: *Industrial Chemistry & Materials* 1.3, pp. 332–342. ISSN: 2755-2608, 2755-2500. DOI: 10. 1039/D3IM00036B. URL: https://xlink.rsc.org/?DOI = D3IM00036B (visited on 2025-04-15).
- Zhang, Tongtong, Joao Uratani, Yixuan Huang, Lejin Xu, Steve Griffiths, and Yulong Ding (2023-04). "Hydrogen liquefaction and storage: Recent progress and perspectives". en. In: *Renewable and Sustainable Energy Reviews* 176, p. 113204. ISSN: 13640321. DOI: 10.1016/j.rser.2023.113204. URL: https://linkinghub.elsevier.com/retrieve/pii/S1364032123000606 (visited on 2025-04-15).